Solution-Processible Bipolar Triphenylamine-Benzimidazole Derivatives for Highly Efficient Single-Layer Organic Light-Emitting Diodes

Ziyi Ge,[†] Teruaki Hayakawa,[†] Shinji Ando,[†] Mitsuru Ueda,[†] Toshiyuki Akiike,[‡] Hidetoshi Miyamoto,[‡] Toru Kajita,[‡] and Masa-aki Kakimoto*,[†]

Department of Organic & Polymeric Materials, Tokyo Institute of Technology, Ookayama 2-12-1, Meguro-ku, Tokyo 152-8552, Japan, and Display Research Laboratories, JSR Corporation, 100 Kawajiri-cho, Yokkaichi, Mie 510-8552, Japan

Received December 12, 2007. Revised Manuscript Received January 20, 2008

Two solution-processible bipolar molecules, tris(3′-(1-phenyl-1*H*-benzimidazol-2-yl)biphenyl-4-yl)amine (TBBI) and tris(2-methyl-3′-(1-phenyl-1*H*-benzimidazol-2-yl)biphenyl-4-yl)amine (Me-TBBI), bearing both hole-transporting triphenylamine and electron-transporting benzimidazole moieties were newly prepared. TBBI and Me-TBBI possess excellent thermal stability with high glass-transition temperature (T_g) of 148 and 144 °C, and the decomposition temperatures (T_d) of 552 and 515 °C in nitrogen, respectively. They exhibit good solubility in common solvents due to the metastructured and star-shaped configuration allowing a solution processing. TBBI and Me-TBBI were employed to fabricate phosphorescent organic light-emitting diodes (OLEDs) as the host materials doped with the guest of $Ir(ppy)_3$ by spin coating with a single-layer structure. The solution-processed Me-TBBI device exhibited an improved performance relative to TBBI arising from the complete charge localization of HOMO and LUMO and an increase in the singlet–triplet (S_0-T_1) energy gap. The performance of spin-coated Me-TBBI device (16400 cd m^{-2}, 27.4 cd A^{-1}, 4.5 lm W^{-1}) is outstanding with respect to other work for fully solution-processed OLEDs with the similar single-layer structure.

Introduction

Considerable studies have been made on organic light-emitting diodes (OLEDs) for their potential applications in the next generation full-color displays as a promising alternative to the conventional Liquid Crystal Displays (LCD).[1,2] Recently, phosphorescent OLEDs have attracted much attention since phosphorescence harvests both singlet and triplet excited states, suggesting the potential for approaching a maximum external quantum efficiency of nearly 100%. Numerous high-performance phosphorescent OLDs with great luminescence and high efficiency have been reported, of which most are based on the small molecule devices fabricated by multilayer vacuum thermal evaporation techniques.[3–5]

On the other hand, to balance the charge recombination efficiency, one promising strategy is to develop bipolar molecules bearing both electron–donating and electron–accepting moieties capable of matching for charge carrier injection and acceptance of both holes and electrons.[6–8] The simplified devices with double-layer or even single-layer structure could be thereby attained by simultaneously supplying electron and hole in the electroluminescent (EL) materials sandwiched between two electrodes.[9–11]

OLEDs have been successfully employed in commercial fields such as the full-color displays and solid light sources, whereas it is restricted by the low fabrication yield down to 50% arising from the complicated multilayer thermal evaporation techniques. It is generally thought that solution processing such as spin coating or ink-jet printing exhibits promising potentials for the low-cost and large-area flat panel display technology.[12] Hence, development of solution-processible fabrication in OLEDs will offer an attractive alternative to vacuum deposition techniques, if high efficiency can also be simultaneously provided.[13,14] So far, most of the high-performance OLEDs based on small

* Corresponding author. E-mail: mkakimot@o.cc.titech.ac.jp. Tel: 81-3-5734-2429. Fax: 81-3-5734-2875 .
[†] Tokyo Institute of Technology.
[‡] JSR Corporation.

(1) Wolak, M. A.; Delacamp, J.; Landis, C. A.; Lane, P. A.; Anthony, J.; Kafafi, Z. *Adv. Funct. Mater.* **2006**, *16*, 1943.
(2) Li, J.; Liu, D.; Li, Y.; Lee, C. S.; Kwong, H. L.; Lee, S. T. *Chem. Mater.* **2005**, *17*, 1208.
(3) Tsuzuki, T.; Tokito, S. *Adv. Mater.* **2007**, *19*, 276.
(4) Baldo, M. A.; O'Brien, D. F.; You, Y.; Shoustikov, A.; Sibley, S.; Thompson, M. E.; Forrest, S. R. *Nature* **1998**, *395*, 151.
(5) Wong, K.; Chen, Y. M.; Lin, Y. T.; Su, H. C.; Wu, C. C. *Org. Lett.* **2005**, *7*, 5361.
(6) Hancock, J. M.; Gifford, A. P.; Zhu, Y.; Lou, Y.; Jenekhe, S. A. *Chem. Mater.* **2006**, *18*, 4924.
(7) Li, Z. H.; Wong, M. S.; Fukutani, H.; Tao, Y. *Org. Lett.* **2006**, *8*, 4271.
(8) Kulkarni, A. P.; Tonzola, C. J.; Babel, A.; Jenekhe, S. A. *Chem. Mater.* **2004**, *16*, 4556.
(9) Huang, T. H.; Lin, J. T.; Chen, L. Y.; Lin, Y. T.; Wu, C. C. *Adv. Mater.* **2006**, *18*, 602.
(10) Deng, L.; Furuta, P. T.; Garon, S.; Li, J.; Kavulak, D.; Thompson, M. E.; Fréchet, J. M. J. *Chem. Mater.* **2006**, *18*, 386.
(11) Shirota, Y.; Kinoshita, M.; Noda, T.; Okumoto, K.; Ohara, T. *J. Am. Chem. Soc.* **2000**, *122*, 11021.
(12) Zhou, G.; Wong, W. Y.; Yao, B.; Xie, Z.; Wang, L. *Angew. Chem.* **2007**, *119*, 1167.
(13) Gather, M. C.; Köhnen, A.; Falcou, A.; Becker, H.; Meerholz, K. *Adv. Funct. Mater.* **2007**, *17*, 191.

10.1021/cm7035458 CCC: $40.75
Published on Web 03/11/2008

Scheme 1. Synthetic Procedures of TBBI and Me-TBBI

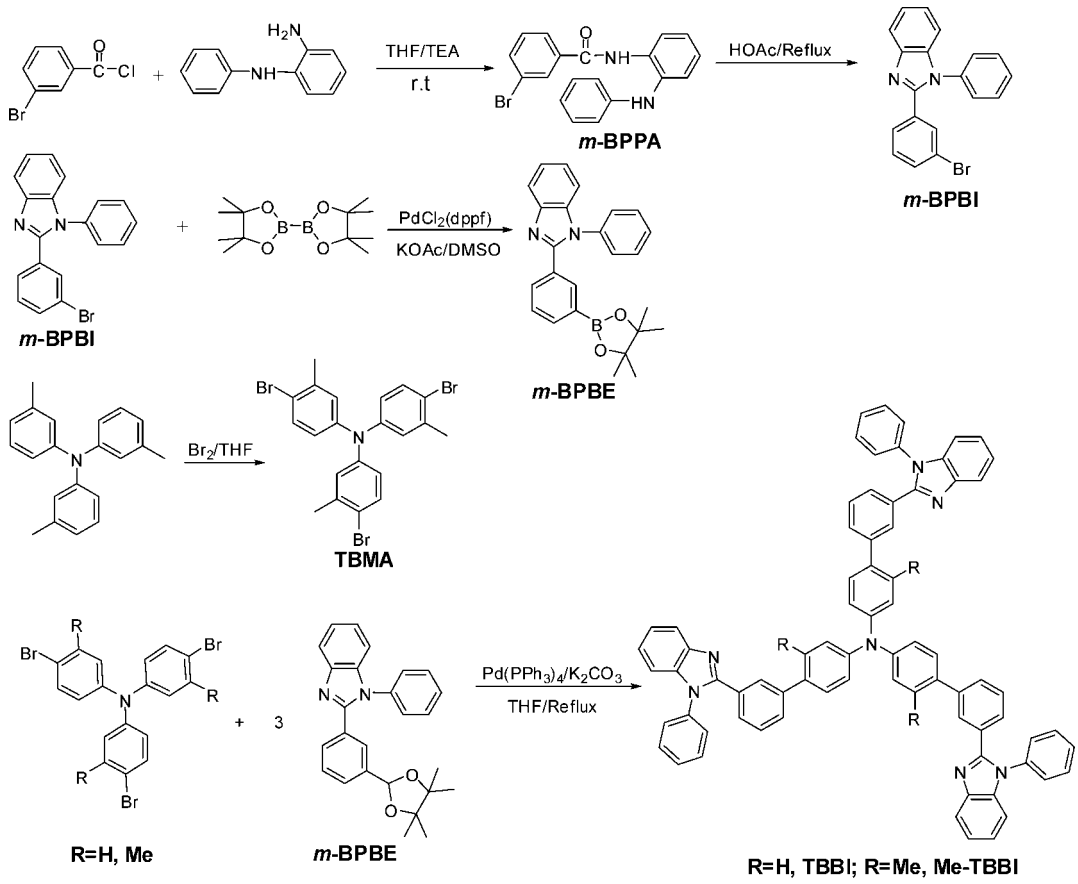

molecules are fabricated by multilayer thermal evaporation even up to six organic layers.[15,16] The layer-by-layer evaporation seems to be a successful technique to afford high efficiency, however, it is limited to many factors such as confine of thermal stable molecules, relatively high cost and time-consuming as well as low process yield. To date, the fabrication of highly efficient solution-processed OLEDs derived from small molecules has not been actively pursued, and those reported based on polymers, large dendriatic molecules, or oligomers are far from satisfactory due to the low luminescence efficiency.[17,18] Of the few highly efficient solution-processed OLEDs reported, most devices were investigated with one or more thermal evaporation layers. Ho et al., as an example, reported a solution-processed devices with a high current efficiency up to 29.8 cd A^{-1}, however, the evaluated device was based on a complicated structure of ITO/PEDOT:PSS (40nm)/Ir-complex:CBP (80nm)/BCP (15nm)/Alq_3 (40nm)/LiF/Al, of which two layers (BCP and Alq_3) were fabricated by vacuum deposition.[19] To the best of our knowledge, fully solution-processed high-performance OLEDs, especially concerning the single-layer ones, were rarely reported in literature, although great requirements are needed.

It is conceivable that the overall cost will be reduced by a more simplified fabrication such as fully solution processing and simple structure with single- or double-layer. Along this respect, in this paper, we report the fully solution-processed OLEDs with single-layer structure based on two bipolar molecules, tris(3′-(1-phenyl-1*H*-benzimidazol-2-yl)biphenyl-4-yl)amine (TBBI) and tris(2-methyl-3′-(1-phenyl-1*H*- benzimidazol-2-yl)biphenyl-4-yl)amine (Me-TBBI), combining both hole-transporting triphenylamine and electron-transporting benzimidazole moieties as shown in Scheme 1. We choose triphenylamine and benzimidazole as the building blocks due to their respective high hole- and electron-transporting mobility.[20–22] In addition, a meta-structured and star-shaped configuration was adopted to improve the solubility and amorphous stability as a result of less molecular packing and large free volume.[23]

TBBI and Me-TBBI exhibited good solubility and high thermal properties. They were fabricated to fully solution-processed single-layer OLEDs by spin coating doped with

(14) Gong, X.; Benmansour, H.; Bazan, G. C.; Heeger, A. J. J. *Phys. Chem. B* **2006**, *110*, 7344.
(15) Bera, R. N.; Cumpstey, N.; Burn, P. L.; Samuel, I. D. W. *Adv. Funct. Mater.* **2007**, *17*, 1149.
(16) Tao, S.; Peng, Z.; Zhang, X.; Wang, P.; Lee, C. S.; Lee, S. T. *Adv. Funct. Mater.* **2005**, *15*, 1716.
(17) Liu, Z.; Zhang, Y.; Hu, Y.; Su, G.; Ma, D.; Wang, L.; Jing, X.; Wang, F. *J. Polym. Sci., Part A: Polym. Chem.* **2002**, *40*, 1122.
(18) Chen, A. C. A.; Wallace, J. U.; Wei, S. K. H.; Zeng, L.; Chen, S. H. *Chem. Mater.* **2006**, *18*, 204.
(19) Ho, C. L.; Wong, W. Y.; Zhou, G. J.; Yao, B.; Xie, Z.; Wang, L. *Adv. Funct. Mater.* **2007**, *17*.
(20) Lu, J.; Xia, P. F.; Lo, P. K.; Tao, Y.; Wong, M. S. *Chem. Mater.* **2006**, *18*, 6194.
(21) Liao, Y. L.; Lin, C. Y.; Wong, K. T.; Hou, T. H.; Huang, W. Y. *Org. Lett.* **2007**, *9*, 4511.
(22) Sonntag, M.; Kreger, K.; Hanft, D.; Strohriegl, P. *Chem. Mater.* **2005**, *17*, 3031.
(23) Li, J. Y.; Liu, D.; Ma, C.; Lengyel, O.; Lee, C. S.; Tung, C. T.; Lee, S. T. *Adv. Mater.* **2004**, *16*, 1538.

fac-tris(2-phenylpyridine)iridium ($Ir(ppy)_3$) as the guest. The EL properties of the devices were investigated, in which the performance of solution-processed Me-TBBI device (16400 cd m^{-2}, 27.4 cd A^{-1}, 4.5 lm W^{-1}) is extensively outstanding among the fully solution-processed single-layer OLEDs ever reported.

Experimental Section

Computational Details. The calculated values of HOMO and LUMO energy levels and the triplet energy gap $\Delta E(T_1-S_0)$ are evaluated by the DFT level of theory with the three-parameter Becke-style hybrid functional (B3LYP), in which the Becke exchange and LYP correlation functionals was adopted in conjunction with the Gaussian basis sets. The 6–31G(d) basis set was used for geometry optimizations of compounds under no constraints, and the 6–311G(d,p) was used for calculations of molecular orbital energies (HOMO and LUMO) and total energies of molecules. A value of $\Delta E(T_1-S_0)$ was calculated as a difference between the total energies at the first excited triplet state (T_1) and the ground singlet state (S_0). The calculated values and the optimized dihedral angles shown in Figure 7 were performed using the software package of Gaussian-03 (Rev.C02 and D01) installed on a Compaq Alpha server GS-320 in the Global Science and Computing Center, Tokyo Institute of Technology.

Measurements. ^1H NMR and ^{13}C NMR measurements were carried out by a JEOL JNM-AL 300 MHz spectrometer in $CDCl_3$, or DMSO-d_6. Matrix assisted laser desorption ionization time of flight mass spectrometry (MALDI-TOF mass) was taken on a Shimazu AXIMA-CFR mass spectrometer. The spectrometer was equipped with nitrogen laser ($\lambda = 337$ nm) and with pulsed ion extraction. The operation was performed at an accelerating potential of 20 kV by a linear-positive ion mode. Samples for MALDI-TOF mass were prepared by casting the matrix compound (dithranol) onto the slide. Column (flash) chromatography was performed using 32–63 um silica gel. Absorption spectra were measured on a HP-8453 diode array spectrometer. Emission spectra were measured on an Aminco-Bowman Series 2 luminescence spectrometer. Electroluminescence spectra were obtained using a PTI QM-2001–4 spectrophotometer. Current–voltage characteristics of the OLEDs were measured using a HP4155A semiconductor parameter analyzer (Yokogawa Hewlett-Packard Tokyo). The luminance was simultaneously measured using a model 370 optometer (UDT instruments, Baltamore, MD).

The experimental values of HOMO levels were determined with a Riken AC-2 photoemission spectrometer (PES), and those of LUMO (S_1) and T_1 levels were estimated from the UV and phosphorescence spectra.

Fabrication of OLEDs. To illustrate the EL properties of the new hosts, single-layer devices using TBBI and Me-TBBI doped with 6% mole $Ir(ppy)_3$ as the emissive layer have been fabricated. In a general procedure, indium−tin oxide (ITO)-coated glass substrates were cleaned sequentially in ultrasonic baths of a 2-propanol/deionized water (1:1 volume) mixture, toluene, deionized water, and acetone before it was dried and treated with UV ozone. A 20 nm poly(ethylenedioxythiophene):poly(styrenesulfonate) (PEDOT:PSS) was spin-coated onto the ITO substrate from the 1 wt % aqueous PEDOT:PSS solution and dried at 140 °C for 1 h under vacuum. A 70 nm thick layer of TBBI or Me-TBBI doped with 6% mole $Ir(ppy)_3$ was later spin-coated from chloroform solution onto the PEDOT:PSS layer and dried at 60 °C for 4 h under vacuum. Twenty nm Cs:BCP (1:1) layer were deposited followed by an 100 nm thick aluminum layer as the cathode. For comparison purpose, the emitting lay of TBBI was also fabricated by vacuum evaporation with a structure similar to that described above.

Synthetic Procedures of TBBI and Me-TBBI. *3-Bromo-N-(2-(phenylamino)phenyl)benzamide (m-BPPA).* The mixture of 3-bromobenzoyal chloride (6.049 g, 27.5 mmol), *N*-phenylbenzene-1,2-diamine (5.079 g, 27.5 mmol), triethylamine (4 mL), and dried THF (80 mL) was stirred for 24 h at room temperature. The solution was poured into water (100 mL) and extracted with dichloromethane. After the solvent was removed, the crude product was recrystallized from methanol and THF to afford a gray solid. Yield: 8.22 g, 81.2%. ^1H NMR (DMSO-d_6, 300 MHz, ppm): 9.84 (s, 1H), 8.04 (s, 1H), 7.87–7.90 (d, 1H), 7.74–7.77 (d, 1H), 7.42–7.52 (m, 3H), 7.28–7.31 (d, 1H), 7.13–7.21 (m, 3H), 6.92–7.01 (m, 3H), 6.76–6.81 (t, 1H). ^{13}C NMR (DMSO-d_6, 77 MHz, ppm): 166.1, 143.9, 138.6, 136.3, 132.7, 131.2, 129.1, 128.9, 128.6, 127.5, 126.1, 125.8, 121.6, 120.1, 119.4, 119.2, 116.2. MALDI-TOF mass (*m*/*z*): 367 (M^+).

2-(3-Bromophenyl)-1-phenyl-1H-benzimidazole (m-BPBI). *m*-BPPA (3.672 g, 10.0 mmol) was refluxed in acetic acid (35 mL) for 12 h before the solvent was removed to give a gray solid. Yield: 3.457 g, 99.0%. ^1H NMR (DMSO-d_6, 300 MHz, ppm): 7.79–7.81 (d, 1H), 7.60–7.65 (t, 2H), 7.31–7.48 (m, 10H). ^{13}C NMR (DMSO-d_6, 77 MHz, ppm): 150.0, 142.3, 137.0, 136.0, 132.2, 131.9, 131.6, 130.4, 130.0, 129.0, 127.8, 127.5, 123.6, 122.9, 121.4, 119.5, 110.5. MALDI-TOF mass (*m*/*z*): 349 (M^+).

1-Phenyl-2-(3-(4,4,5,5-tetramethyl-1,3-dioxolan-2-yl)phenyl)-1H-benzoimidazole (m-BPBE). A mixture of *m*-BPBI (1.048 g, 3.0 mmol), 4,4,4′,4′,5,5,5′,5′-octamethyl-2,2′-bi(1,3,2-dioxaborolane) (0.838 g, 3.3 mmol), diphenylphosphineferrocene palladium dichloride ($PdCl_2$(dppf), 0.073 g, 0.09 mmol), KOAc (0.883 g, 9.0 mmol), and DMSO (18 mL) was stirred at 80 °C for 6 h. After cooling to room temperature, the mixture was extracted with ethyl acetate followed by purification by column chromatography on silica gel with ethyl acetate/hexane (v/v, 1:3) as the eluent to offer a white solid. Yield: 1.071 g, 90.0%. ^1H NMR (DMSO-d_6, 300 MHz, ppm): 8.07 (s, 1H), 7.77–7.80 (d, 1H), 7.63–7.65 (d, 1H), 7.54–7.57 (m, 3H), 7.39–7.43 (m, 3H), 7.24–7.31 (m, 3H), 7.16–7.17 (d, 1H), 1.27 (s, 12H). ^{13}C NMR (DMSO-d_6, 77 MHz, ppm): 151.5, 142.5, 137.0, 136.4, 135.6, 135.1, 131.4, 130.0, 129.2, 128.8, 127.7, 127.5, 123.3, 122.7, 119.3, 110.4, 83.8, 24.7. MALDI-TOF mass (*m*/*z*): 396 (M^+). Elemental anal. Calcd for $C_{25}H_{25}BN_2O_2$: C, 75.77; H, 6.36; N, 7.07. Found: C, 75.58; H, 6.31; N, 7.13.

Tris(3′-(1-phenyl-1H-benzimidazol-2-yl)biphenyl-4-yl)amine (TBBI). In a typical Suzuki-coupling reaction, a mixture of *m*-BPBE (1.020 g, 2.57 mmol), tris(4-bromophenyl)amine (0.375 g, 0.77 mmol), tetrakis(triphenylphosphine) palladium (0.036 g, 0.03 mmol), potassium carbonate (2M, 3.85 mL, 7.7 mmol) ,and THF (20 mL) was added into a 50 mL flask and refluxed for 48 h under argon, which was then extracted with dichloromethane and dried over anhydrous Na_2SO_4. After evaporation the residue was purified by column chromatography on silica gel with dichloromethane/diethyl ether (10:1) as the eluent followed by reprecipitation in methanol to give a yellow solid. Yield: 0.438 g, 54.2%. ^1H NMR ($CDCl_3$, 300 MHz, ppm): 7.74–7.77 (d, 3H), 7.67 (s, 3H), 7.30–7.39 (m, 15H), 7.06–7.13 (m, 18H), 7.05–7.07 (m, 6H), 6.93–6.96 (d, 6H). ^{13}C NMR ($CDCl_3$, 77 MHz, ppm): 170.4, 151.6, 146.3, 142.3, 139.8, 136.6, 136.5, 134.2, 129.6, 129.5, 128.3, 128.1, 127.3, 127.1, 127.0, 123.8, 123.0, 122.6, 119.2, 109.9. FT-IR (KBr, cm^{-1}): 3420, 3045, 1597, 1505, 1475, 1451, 1376, 1323, 1277, 1188, 835, 746. MALDI-TOF mass (*m*/*z*): 1050 (M^+). Elemental anal. Calcd for $C_{75}H_{51}N_7$: C, 85.77; H, 4.89; N, 9.34. Found: C, 85.47; H, 4.80; N, 9.33.

Tris(4-bromo-3-methylphenyl)amine (TBMA). Tri-*m*-tolylamine (1.100 g, 3.80 mmol) was dissolved in dried dichloromethane (20 mL) at –5 °C under argon, to which bromine (1.838 g, 11.50 mmol) was added dropwise in 0.5 h and stirred for 0.5 h. After removing

Table 1. Physical Properties of TBBI and Me-TBBI

compd	λ_{abs}[a] (nm)	λ_{PL}[b] (nm)	T_g[c], T_d[d] (°C)	HOMO/LUMO$_{cal}$ $\Delta\epsilon$ (eV)	HOMO/LUMO$_{exp}$ $\Delta\epsilon$ (eV)	ΔE $(T_1-S_0)_{calcd/exp}$ (eV)
TBBI	295, 352	510	148, 552	5.25/1.52, 3.73	5.49, 2.41, 3.08	2.99, 2.59
Me-TBBI	302	470	144, 515	5.00/1.35, 3.65	5.37, 2.19, 3.18	3.09, 2.76

[a] Absorption maximum, measured in chloroform. [b] PL maximum, measured in chloroform. [c] Glass-transition temperature. [d] Thermal decomposition temperature.

the solvent the solid was refluxed in hot methanol (50 mL) for 1 h and recrystallized from methanol and THF. Yield: 0.70 g, 35.0%. ^{1}H NMR ($CDCl_3$, 300 MHz, ppm): 7.34–7.37 (d, 3H), 6.89 (s, 3H), 6.71–6.74 (d, 3H), 2.28 (s, 9H). ^{13}C NMR ($CDCl_3$, 77 MHz, ppm): 146.4, 139.0, 133.0, 126.2, 123.1, 118.4, 23.0.

Tris(2-methyl-3′-(1-phenyl-1H-benzimidazol-2-yl)biphenyl-4-yl)amine (Me-TBBI). Me-TBBI was prepared with the same cross-coupling procedure as TBBI from *m*-BPBE and TBMA. Yield: 1.53 g, 50.5%. ^{1}H NMR ($CDCl_3$, 300 MHz, ppm): 7.87–7.90 (d, 3H), 7.50–7.55 (m, 15H), 7.33–7.36 (m, 15H), 7.24–7.26 (m, 6H), 6.91–6.93 (m, 9H), 2.01 (s, 9H). ^{13}C NMR ($CDCl_3$, 77 MHz, ppm): 152.4, 146.7, 142.8, 141.6, 137.1, 137.0, 136.2, 135.4, 130.5, 130.4, 129.9, 129.6, 128.5, 128.1, 127.6, 127.4, 125.5, 123.3, 123.0, 121.5, 119.8, 110.4, 20.3. FT-IR (KBr, cm^{-1}): 3423, 3053, 1596, 1505, 1478, 1452, 1379, 1323, 1267, 745, 699. MALDI-TOF mass (*m*/*z*): 1092 (M^+). Elemental anal. Calcd for $C_{78}H_{57}N_7$: C, 85.76; H, 5.26; N, 8.98. Found: C, 85.39; H, 5.13; N, 9.01.

Results and Discussion

Synthesis of TBBI and Me-TBBI. Scheme 1 illustrates the synthetic procedures for TBBI and Me-TBBI. First, 3-bromo-*N*-(2-(phenylamino)phenyl)benzamide (*m*-BPPA) was prepared from the condensation of 3-bromobenzoyl chloride and *N*-phenylbenzene-1,2-diamine catalyzed by triethylamine (TEA) in THF with 81.2% yield. The benzimidazole, 2-(3-bromophenyl)-1-phenyl-1*H*-benzimidazole (*m*-BPBI) were synthesized by the cyclization of *m*-BPPA in acetic acid at reflux, which were then converted to the arylboronic ester of 1-phenyl-2-(3-(4,4,5,5-tetramethyl-1,3-dioxolan-2-yl)phenyl)-1*H*- benzimidazole (*m*-BPBE) catalyzed by $PdCl_2$(dppf) in the presence of K_2CO_3 and DMSO. Tri*m*-tolylamine was brominated to tris(4-bromo-3-methylphenyl)amine (TBMA) with bromine in dichloromethane. The Suzuki cross-coupling reactions of tris(4-bromophenyl) amine and TBMA with the arylboronic ester *m*-BPBE led to TBBI and Me-TBBI, respectively. Both compounds TBBI and Me-TBBI were isolated and purified by column chromatography on silica gel, followed by reprecipitation from methanol with good yields and high purity. ^{1}H and ^{13}C NMR, IR, MALDI-TOF mass spectrometry, and elemental analysis were employed to confirm the chemical structures of above-mentioned compounds as described in the experimental section.

Physical Properties of TBBI and Me-TBBI. TBBI and Me-TBBI can readily dissolve in common organic solvents, such as chloroform, 1,2-dichloroethane, THF, toluene, anisole, and cyclohexanone owing to the low ordered molecular arrangement arising from the meta-structured and star-shaped configuration, which enables the preparation of uniform thin films by solution processing such as spin coating.

The thermal properties of TBBI and Me-TBBI were investigated by differential scanning calorimetry (DSC) and thermal gravimetric analysis (TGA) measurements. As shown in Table 1, TBBI and Me-TBBI possess high T_g of 148 and 144 °C, respectively, which is significantly higher than the commonly used hole-transporting material of 1,4-bis(1-naphthylphenylamino)biphenyl (NPB, T_g: 98 °C). The TGA measurements show the compounds are thermally stable up to 510 °C with the decomposition temperatures (T_d) in the range of 515–552 °C in nitrogen. Thermal and morphological stability of organic EL materials play an important role in OLEDs. The excellent thermal stability with high T_d and T_g readily indicates high-stability OLEDs and high morphological stability, which is favorable to improve OLEDs performance and lifetime during operation.

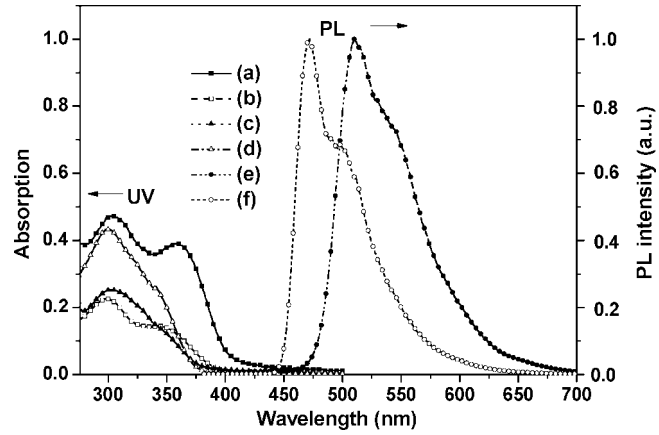

Figure 1. UV spectra of TBBI and Me-TBBI in chloroform or films and PL spectra in chloroform. (a) TBBI solution, (b) TBBI film, (c) Me-TBBI solution, (d) Me-TBBI film, (e) PL of TBBI, (f) PL of Me-TBBI.

Photophysical Properties of TBBI and Me-TBBI. The photophysical properties of TBBI and Me-TBBI were measured using UV–visible absorption and photoluminescence (PL) spectra as shown in Figure 1 and Table 1. No significant changes in the UV spectra were observed on going from solutions to corresponding films, suggesting a weak intermolecular interaction. TBBI has its lowest-energy absorption band centered at 352 nm associated with the charge transfer (CT) type $\pi-\pi^*$ transition from the HOMO located at the electron-donating triphenylamine moiety to the LUMO located at the electron-accepting benzimidazole moiety. An additional band with high intensity at 295 nm is attributed to the locally excited (LE) $\pi-\pi^*$ transition at the triphenylamine moiety. Note that only one broad absorption band is observed for Me-TBBI, which is caused by the significant blue shift of the CT ($\pi-\pi^*$) transition toward the LE ($\pi-\pi^*$) transition. The PL emission maxima of TBBI and Me-TBBI are observed around 510 and 470 nm, respectively, and the emission of Me-TBBI are blue-shifted by 40 nm relative to TBBI due to the incorporation of methyl groups that interrupts the π-conjugation between triphenylamine and benzimidazole units.

As shown in Table 1, the experimental HOMO is 5.49 eV for TBBI and 5.37 eV for Me-TBBI, while the LUMO levels are 2.41 and 2.19 eV, individually, which is in

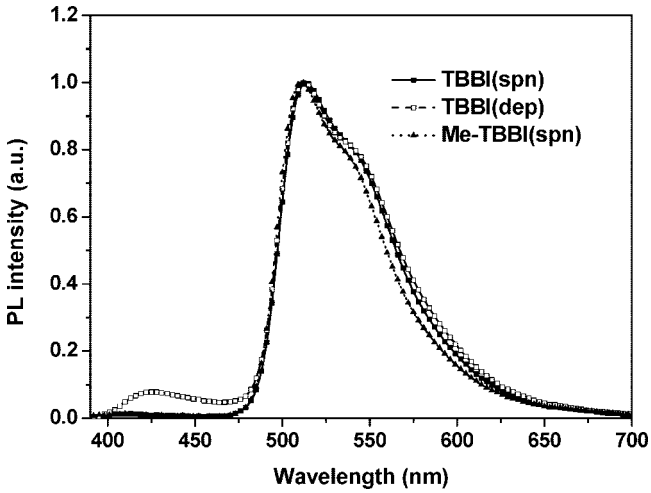

Figure 2. EL spectra of the devices.

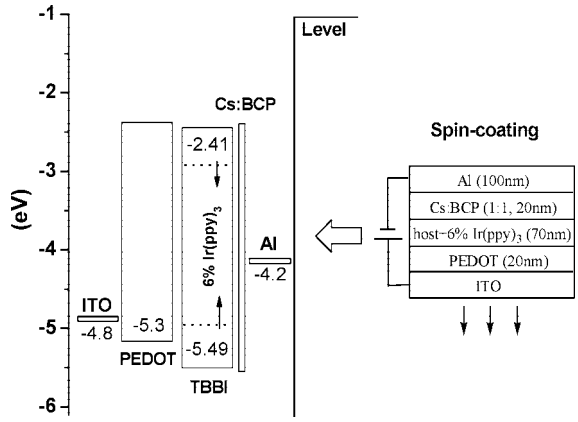

Figure 3. Energy diagram of TBBI in device fabrication. The device structure is incorporated.

excellent agreement with the calculated values (5.25 and 5.00 eV for the HOMO, and 1.52 and 1.35 for the LUMO of TBBI and Me-TBBI, respectively).

Light-Emitting Diodes. OLEDs based on TBBI and Me-TBBI were fabricated on ITO with the single-layer structure of ITO/PEDOT:PSS (20 nm)/TBBI or Me-TBBI + 6% mol $Ir(ppy)_3$ (70nm)/Cs:BCP (1:1) (20 nm)/Al (100 nm) by spin coating. As comparison, a vacuum-deposited TBBI device was also fabricated. TBBI or Me-TBBI doped with $Ir(ppy)_3$ served as the emitting layer and Cs:BCP/Al act as the cathode while ITO served as the anode. It was named a single-layer structure base on the fact that the well-known PEDOT:PSS was used as a smoothing layer for ITO, and no additional charge-transporting layers were utilized in the structure.[24]

The EL spectra (Figure 2) of devices indicate the emissions fall in green region with the typical green luminescence around 510 nm dominated by the guest $Ir(ppy)_3$, implying the transferred triplet exitons are well confined on $Ir(ppy)_3$, which can be attributed to the balance of energy levels. The EL spectra of vacuum deposited TBBI device exhibited no obvious difference with respect to the spin-coated one because of the high morphological stability arising from the excellent thermal stability. By examination of the representative energy-level diagram for TBBI device in Figure 3, it can be seen that the HOMO level of PEDOD:PSS (5.3 eV as determined) is close to that of TBBI (HOMO, 5.49 eV),

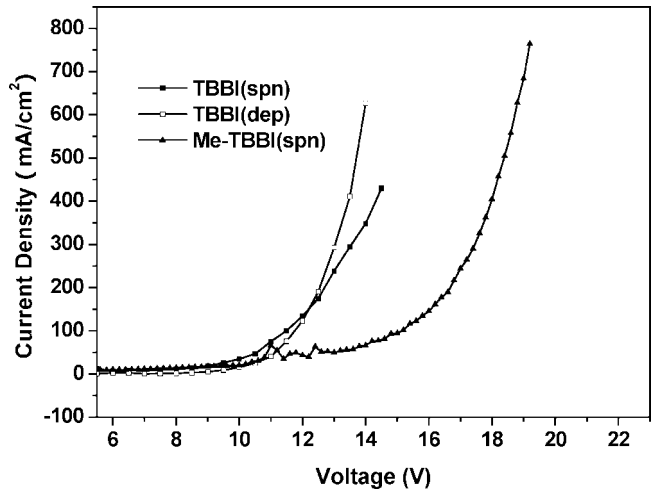

Figure 4. Current density versus voltage characteristics for the devices.

which reduces the HOMO energy level barrier between ITO (4.8 eV) and TBBI and improves the hole injection consequently, indicating the PEDOT:PSS buffer layer is necessary in the structure. The HOMO level of TBBI lies about 0.41 eV lower than $Ir(ppy)_3$ and LUMO about 0.5 eV higher, implying that both holes and electrons would be trapped on TBBI in the blend. From the current–voltage ($I-V$) curves shown in Figure 4, TBBI exhibited lower turn on voltages compared with Me-TBBI, which may be attributed to that Me-TBBI possesses a wider HOMO–LUMO energy band ($\Delta\epsilon$, 3.18 eV) than TBBI (3.08 eV) causing the increase in the driving voltage.

EL properties of the devices are studied and summarized in Table 2. Figure 5 showed the current–luminance ($I-L$) characteristics of TBBI and Me-TBBI devices. The solution processed devices exhibited excellent performance with the maximum luminance and current efficiency of 12800 cd m^{-2} and 4.3 cd A^{-1} for TBBI, which is a little lower as compared with the vacuum-deposited one, and 16400 cd m^{-2} and 27.4 cd A^{-1} for Me-TBBI, respectively. The power and current efficiency at 200 cd m^{-2} exhibited as high as 0.3 lm W^{-1} and 0.8 cd A^{-1} for TBBI, 4.4 lm W^{-1} and 26.8 cd A^{-1} for Me-TBBI, individually. One should note that the devices are entirely solution-processed with a single-layer structure without additional optimizations except for a smoothing PEDOT:PSS layer. The performance of solution-processed Me-TBBI was much higher than those devices with similar fabrication, e.g., reported by Ding et al. (0.30–0.60 cd A^{-1} for solution-processed devices with the structure of ITO/PEDOT:PSS (50nm)/Dendrimers/Ca (10 nm)/Al).[25] To the best of our knowledge, the performance of the spin-coated Me-TBBI device (16400 cd m^{-2} and 27.4 cd A^{-1}) is outstanding in solution-processed devices with a single-layer structure and even comparable to some vacuum-deposited ones ever reported.

The voltage−current efficiency curves were shown in Figure 6, in which Me-TBBI reached the maximum current efficiency at a driving voltage of 19 V. It is interesting to

(24) Cheng, J. A.; Chen, C. H.; Liao, C. H. *Chem. Mater.* **2004**, *16*, 2862.
(25) Ding, J.; Gao, J.; Cheng, Y.; Xie, Z.; Wang, L.; Ma, D.; Jing, X. *Adv. Funct. Mater.* **2006**, *16*, 575.
(26) Jeon, J. Y.; Park, T. J.; Jeon, W. S.; Par, J. J.; Jang, J.; Kwon, J. H.; Lee, J. Y. *Chem. Lett.* **2007**, *36*, 1156.

Table 2. EL Properties of the OLEDs

host	device	V_{on}[a]	L_{max}[b] (cd m^{-2})	$\eta_{p,max}$[c]	$\eta_{c,max}$[d] (cd A^{-1})	η_p[e] (lm W^{-1})	η_c[e] (cd A^{-1})	CIE[f]
TBBI	Spn[h]	6.7	12 800	1.1	4.3	0.3	0.8	0.29, 0.63
	Dep[i]	6.4	20 000	2.2	6.1	2.2	6.1	0.29, 0.58
Me-TBBI	Spn	13.1	16 400	4.5	27.4	4.4	26.8	0.26, 0.55

[a] Turn-on voltage. [b] Maximum luminance. [c] Maximum power efficiency. [d] Maximum current efficiency. [e] Power efficiency and current efficiency at 200 cd m^{-2}, respectively. [f] Commission Internationale de l'Eclairage coordinates. [h] Spin-coating. [i] Vacuum-deposited TBBI device was fabricated as comparison.

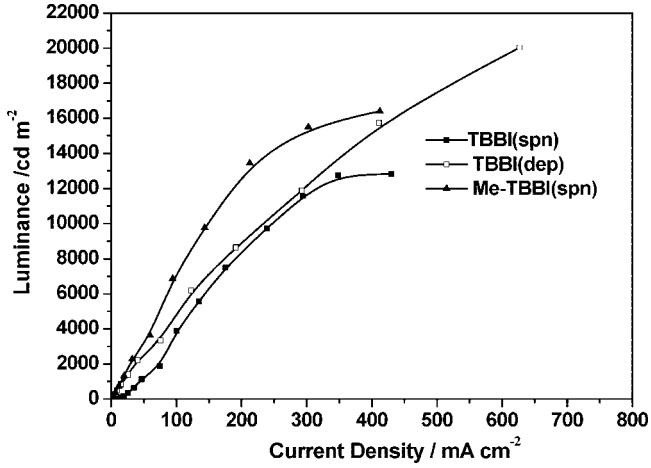

Figure 5. Luminance versus current density characteristics for the devices.

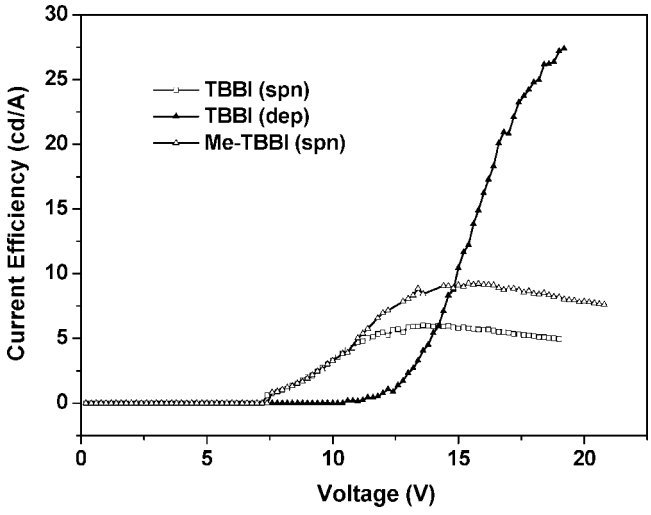

Figure 6. Current efficiency versus voltage characteristics for the devices.

note that device derived from Me-TBBI incorporated with methyl group exhibited much enhanced efficiency relative to that of TBBI by 27.4 cd A^{-1} to 4.3 cd A^{-1}. We attributed this drastic improvement to the combined effects of the enhancement in the localization and separation of charges and the increase in triplet energy gap $\Delta E(T-S_0)$ of the host materials. As shown in Figure 7, the calculation results showed that Me-TBBI exhibited the complete separation of HOMO and LUMO at their respective hole- and electron-transporting, whereas TBBI exhibits lesser segregation of HOMO and LUMO. Usually, holes and electrons in OLEDs are transferred through the individual HOMO and LUMO levels.[26] The complete localization of HOMO and LUMO means the HOMO → LUMO transition becomes a typical charge transfer (CT) transition, which is desirable for the

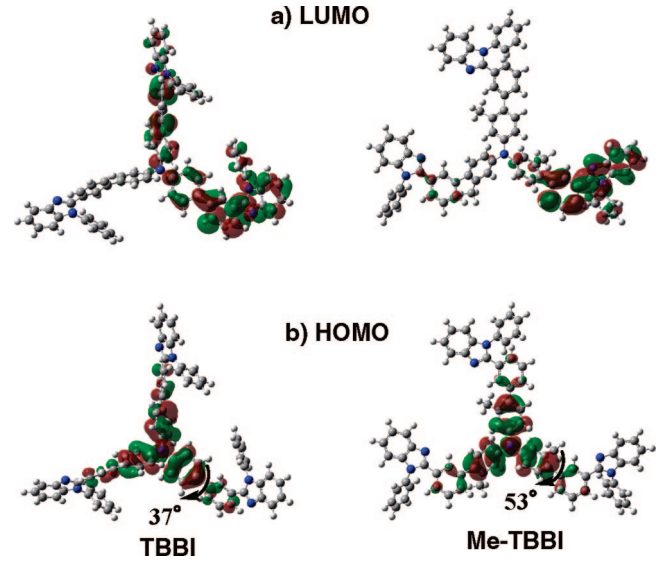

Figure 7. Calculated spatial distributions of LUMO and HOMO of TBBI and Me-TBBI. The values of optimized dihedral angles φ at the biphenyl linkages are incorporated.

efficient energy transfer. Furthermore, the triplet energy gap of Me-TBBI is significantly higher than TBBI by 2.76 to 2.59 eV, which is caused by the more twisted structure in the arms of Me-TBBI than that in TBBI. As shown in Figure 7, the optimized dihedral angles φ at the biphenyl linkage increased from 37 (TBBI) to 53° (Me-TBBI) according to DFT calculations, which lead to a decrease in the coupling between the electron-donator and -acceptor moieties. A large triplet energy gap $\Delta E(T-S_0)$ is preferable to prevent the back excitation transfer from the guest molecules of heavy metal complexes to the host materials.

Conclusion

Two metastructured and star-shaped host molecules TBBI and Me-TBBI with desired bipolar character containing hole-transporting triphenylamine and electron-transporting benzimidazole moieties were newly designed and successfully synthesized. Single-layer phosphorescent OLEDs based on TBBI or Me-TBBI doped with guest $Ir(ppy)_3$ were fabricated by spin coating technique, which exhibited superior luminance efficiency. Me-TBBI exhibits higher efficiency than TBBI arising from the complete localization and separation of charges and the increased triplet energy gap relative to those of TBBI, which originates from the decreased π-conjugation interrupted by the methyl group. The performance of solution-processed single-layer Me-TBBI device (16400 cd m^{-2}, 27.4 cd A^{-1}, 4.5 lm W^{-1}) is outstanding compared to other similar work, indicating great commercial potentials.

CM7035458